HEAVY-ION PHYSICS HIGHLIGHTS FROM ATLAS*

Iwona Grabowska-Bold ⓘ

on behalf of the ATLAS Collaboration

AGH University of Krakow, al. Mickiewicza 30, 30-059 Kraków, Poland

Recent measurements from the heavy-ion physics programme from the ATLAS experiment at the LHC are reviewed. They include azimuthal flow at high transverse momenta (p_T), p_T fluctuations in lead–lead (Pb+Pb) and xenon–xenon (Xe+Xe) collisions, jet-radius dependence of di-jet asymmetry, and an observation of top-quark pair production in proton–lead (p+Pb) and Pb+Pb systems. Results of a search for a diffusion wake in γ–jet events are also discussed. Moreover, results from ultra-peripheral collisions for photonuclear di-jet production and a search for magnetic monopoles are presented.

1. Introduction

The ATLAS experiment [1] at the Large Hadron Collider (LHC) is designed and built to collect and study proton–proton (pp) collisions. It has been successfully recording data since 2010. On average, four weeks per year of the beam time are devoted to the heavy-ion (HI) physics programme, with nucleus–nucleus collisions occurring at the interaction points. In particular, in the second period of the LHC operations, so-called Run 2, Pb+Pb, p+Pb, and Xe+Xe collisions were recorded by the experiments at the centre-of-mass energy per nucleon pair of $\sqrt{s_{NN}} = 5.02$ TeV, 8.16 TeV, and 5.44 TeV, respectively. The third LHC data-taking period (Run 3) started in 2022 and is still in progress. The centre-of-mass energy of Pb+Pb collisions in Run 3 is slightly increased to $\sqrt{s_{NN}} = 5.36$ TeV compared to Run 2.

In this report, a selection of recent ATLAS measurements from the Run 2 HI programme is reported. Results from the first measurement based on Run 3 Pb+Pb data collected in 2023 are also discussed.

---

* Presented at the 31$^{\text{st}}$ Cracow Epiphany Conference on the *Recent LHC Results*, Kraków, Poland, 13–17 January, 2025.

2. Insights into the QGP

The HI programme at the LHC focuses on the measurements of the quark–gluon plasma (QGP) and studies of its properties. The QGP is an ultra-hot and ultra-dense state of matter in which quarks and gluons are no longer confined in colour-neutral hadrons. To understand the properties of the QGP, a variety of probes are utilised. The hydrodynamic expansion of the QGP induces a significant boost to the p_T of the final-state particles. This boost transforms the shape anisotropies and size variations in QGP's initial state into final-state anisotropies known as anisotropic flow and variations in the average p_T in each event. In the following, this phenomenon is studied by ATLAS with unprecedented precision. To probe the QGP at short distances, high-p_T probes such as jets are used. Jets traversing the QGP experience *jet quenching*, characterised by a reduction in the overall jet energy compared to expectations from pp collisions. Historically, the jet-quenching phenomenon was discovered by a direct observation of di-jet asymmetry [2] at the LHC. In the following, new precise results for di-jet production in HI collisions from ATLAS are also discussed, and traces of jets impact on anisotropy of charged hadrons.

2.1. Soft physics with charged particles

Elliptic (v_2) and triangular (v_3) azimuthal anisotropy coefficients for charged particles produced in Pb+Pb collisions at 5.02 TeV using a data set corresponding to an integrated luminosity of 435 μb^{-1} collected in 2018 are measured by ATLAS [3]. The focus of the analysis is the precise extraction of v_2 and v_3 at high p_T above 10 GeV and up to 400 GeV where the origin of the flow is attributed to jet energy loss. The measurement is done in intervals of Pb+Pb collision centrality, 0–60%, using the scalar product and multi-particle cumulant methods. These have different sensitivity to event-by-event fluctuations and non-flow effects in the measurements of azimuthal anisotropies. Figure 1 shows v_2 (left) and v_3 (right) as a function of charged-particle p_T for the two methods for the 10–20% centrality bin. Positive values of v_2 are observed up to a p_T of approximately 100 GeV from both methods. Positive values of v_3 are observed up to approximately 25 GeV using both methods, though the application of the three-subevent technique to the multi-particle cumulant method leads to significant changes at the highest p_T. For p_T above 10 GeV, charged particles are predominantly from jet fragmentation. The measurements presented here are sensitive to the path-length dependence of parton energy loss in the QGP produced in collisions.

ATLAS also made further progress in studies of v_n–p_T correlations using Pb+Pb and Xe+Xe collisions [4]. The new measurement is focused on disentangling sources of momentum fluctuations by utilising ultra-central colli-
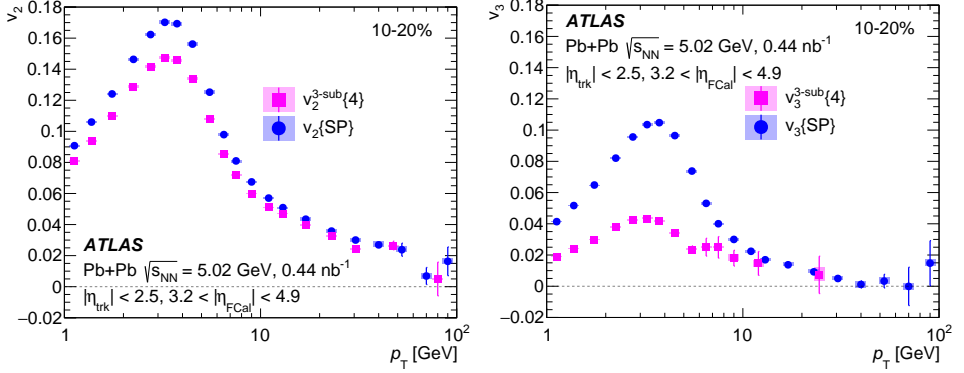
Fig. 1. Elliptic (left) and triangular flow (right) coefficients as a function of charged particle p_T measured using the scalar product and multi-particle cumulant methods [3].

sions (UCC) from the 0–5% or 0–1% classes. Distinguishing between contributions from fluctuations in the size of the nuclear overlap area (geometrical component) and other sources at fixed size (intrinsic component) presents a challenge. In the measurement, these two components are distinguished by measuring the mean, variance, and skewness of the event-averaged transverse momenta of charged particles, $[p_T]$. The left panel of Fig. 2 shows the correlation between the $[p_T]$ and charged-particle multiplicity N_{ch} values averaged over these events for Pb+Pb and Xe+Xe collisions in two p_T ranges for 0–1% UCC. The correlation is observed to be positive and nearly linear, and with similar slopes in both systems. The slope, however, varies with the p_T range selection, reflecting the kinematic sensitivity to the radial flow.
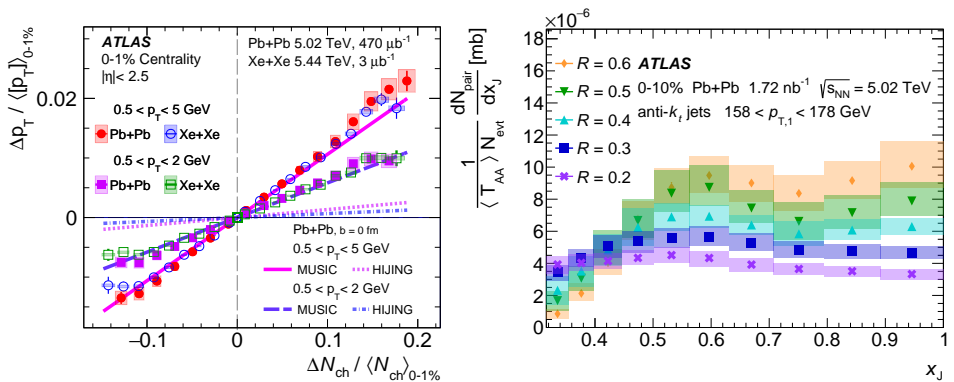

Fig. 2. Left: Correlation between the event-wise average $[p_T]$ and N_{ch} values averaged over events from 0–1% UCC for Pb+Pb and Xe+Xe collisions in two p_T intervals [4]. Right: Absolutely normalised di-jet momentum balance distributions for $R = 0.2$–0.6 jets in the 0–10% centrality interval [7].

The Pb+Pb data are compared to the HIJING model [5], which has no final-state interactions, and the state-of-the-art MUSIC model [6], which includes the full hydrodynamic response of the QGP to its initial-state geometry. The HIJING model grossly underpredicts the slope of the data, while the MUSIC model quantitatively captures the slopes of the correlation observed in the data in both p_T ranges. The MUSIC model with the QGP equation-of-state parameters, speed of sound, and effective temperature set to 0.23 and 222 MeV, respectively, and therefore allowing to indirectly estimate them.

2.2. Hard physics with jets

ATLAS studied the jet-radius dependence of the di-jet momentum balance between leading back-to-back jets in Pb+Pb and pp collisions [7]. Both data sets are recorded at 5.02 TeV. Jets are reconstructed using the anti-k_T algorithm with jet-radius parameters R equal to 0.2, 0.3, 0.4, 0.5, and 0.6. The di-jet momentum balance distributions are constructed for leading jets with p_T from 100 to 562 GeV for $R = 0.2$, 0.3, and 0.4 jets, and from 158 to 562 GeV for $R = 0.5$ and 0.6 jets. The absolutely normalised di-jet momentum balance distributions ($x_J = p_{T,2}/p_{T,1}$, where $p_{T,1}$ and $p_{T,2}$ are leading and sub-leading jets in the event, respectively) are constructed to compare measurements of the di-jet yields in Pb+Pb collisions directly to the di-jet cross sections in pp collisions. The right panel of Fig. 2 shows the x_J distributions for all studied jet R-sizes in the 0–10% centrality class. The x_J distributions in Pb+Pb collisions are broadened compared to those in the pp system (see in Ref. [7]). For $158 < p_{T,1} < 178$ GeV selection, the distributions are nearly flat for $x_J > 0.5$. A peak develops at intermediate x_J values. It becomes weaker as the jet radius decreases. These measurements provide new constraints on jet-quenching scenarios in the QGP.

2.3. Search for a diffusion wake

A measurement of jet-track correlations in γ–jet events, using 1.72 nb^{-1} of Pb+Pb data at 5.02 TeV is performed by ATLAS [8]. Events with energetic γ–jet pairs are selected, where the photon and jet are approximately back-to-back in azimuth. The angular correlation between jets and charged-particle tracks with p_T in the 0.5–2.0 GeV range in the hemisphere opposite to the jet, is measured as a function of their relative pseudorapidity difference, $\Delta\eta(\text{jet}, \text{track})$. In central Pb+Pb collisions, these correlations are predicted to be sensitive to the diffusion wake in the QGP resulting from the lost energy of high-p_T partons traversing the plasma, with a characteristic modification as a function of $\Delta\eta(\text{jet}, \text{track})$ [9]. The correlations are examined with different selections on the jet-to-photon p_T ratio denoted by $x_{J\gamma}$ to select events with different degrees of energy loss. Figure 3 shows a ratio of correlation functions as a function of $\Delta\eta(\text{jet}, \text{track})$ for three different

$x_{\mathrm{J}\gamma}$ intervals in 0–10% centralities. For all three $x_{\mathrm{J}\gamma}$ selections, the results are consistent with unity within uncertainties. No diffusion wake signal is observed within the current sensitivity of the data, and upper limits at the 95% confidence level on the diffusion wake amplitude are established.
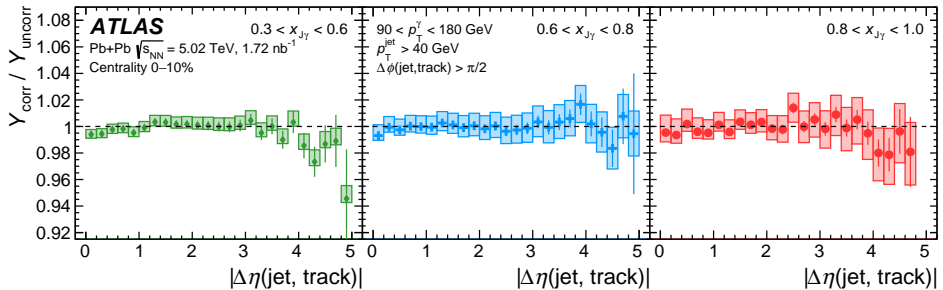

Fig. 3. Ratio of correlation functions as a function of $\Delta\eta(\mathrm{jet},\mathrm{track})$ for three different $x_{\mathrm{J}\gamma}$ intervals in the 0–10% centrality class of Pb+Pb collisions [8].

3. Observation of top quarks in HI collisions

With the high integrated luminosity of p+Pb collisions recorded in 2016, ATLAS measured top-quark pair production ($t\bar{t}$) for the first time [10]. Decay modes with two leptons (di-lepton) or lepton+jet are studied. Electron and muon final states are explored. Using a simultaneous profile likelihood fit in six signal regions (SRs), the signal strength defined as a ratio of the measured-to-predicted cross sections, is extracted. The signal significance exceeds 5σ in all SRs marking a first observation of $t\bar{t}$ production in the di-lepton channel in HI collisions at the LHC. The measurement features the most precise inclusive cross-section value for $t\bar{t}$ production in p+Pb collisions. The nuclear modification factor (R_{pA}) for $t\bar{t}$ production is measured for the first time at the LHC. Its value is shown in the left panel of Fig. 4. The central value of R_{pA} is above unity hinting at the expected enhancement of $t\bar{t}$ production in p+Pb collisions in comparison to the pp system. The relative uncertainty of the measurement amounts to 9% and is dominated by the systematic component due to modelling of $t\bar{t}$ production and background estimation from fake leptons in the lepton+jet channel. R_{pA} is also compared to other measurements and theoretical predictions for the signal process involving different nuclear modifications to PDF (nPDF) sets. A good agreement is found.

ATLAS also measured $t\bar{t}$ production in the full set of Run 2 Pb+Pb collisions with an integrated luminosity of 1.9 nb^{-1} [11]. The di-lepton channel is analysed with opposite-sign and different-flavour leptons ($e\mu$). The same-
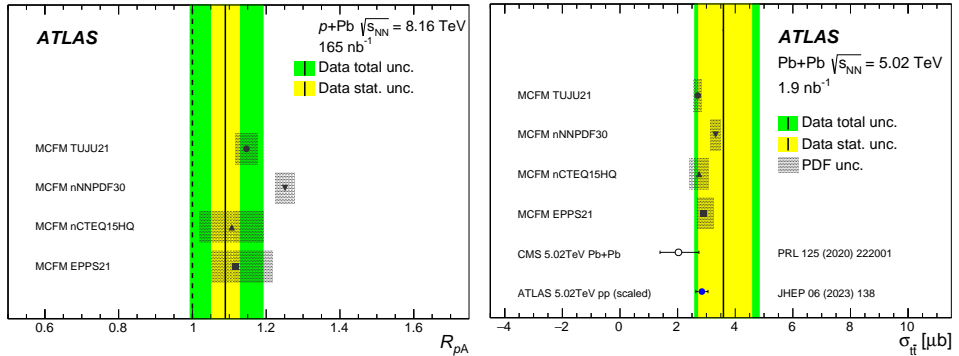
Fig. 4. Left: Nuclear modification factor for $t\bar{t}$ production in p+Pb collisions [10]. Right: Inclusive cross section for $t\bar{t}$ production in Pb+Pb collisions [11].

flavour lepton channels (e^+e^- and $\mu^+\mu^-$) serve as control regions for performance studies. The signal strength is extracted from the profile likelihood fit to the mass distribution of the $e\mu$ system. Its significance amounts to 5σ establishing the first observation of top-quark production in the Pb+Pb system at the LHC. The inclusive cross section for $t\bar{t}$ production is also measured. Its total relative uncertainty amounts to 31% and is dominated by statistical precision. The cross-section value is shown in the right panel of Fig. 4. It is compared to the existing measurements and to theory predictions involving different nPDF sets. A good agreement is found.

4. Ultra-peripheral collisions

With the observation of a rare light-by-light process [12, 13], the ATLAS Collaboration marked the start of the physics programme based on ultra-peripheral collisions (UPC). The UPC occurs when two ion beams pass next to each other with impact parameters slightly larger than two times the nuclear radius. Under such circumstances, the extremely strong electromagnetic fields accompanying nuclear beams might interact. The interaction can be described by the Equivalent Photon Approximation with two quasi-virtual photons ($\gamma\gamma$) or photon–nucleus ($\gamma + A$) collisions. Due to high electric charge associated with each ^{82}Pb nucleus, the UPC cross sections are significantly enhanced in the Pb+Pb system in comparison to pp collisions at the LHC.

4.1. Multi-jet production via $\gamma + A$

ATLAS measured production of di-jet and multi-jet final states in UPC Pb+Pb at $\sqrt{s_{NN}} = 5.02$ TeV using a data set recorded in 2018 with an inte-

grated luminosity of 1.72 nb^{-1} [14]. Photonuclear final states, $\gamma + A$, are selected by requiring a rapidity gap in the photon direction; this selects events where one of the outgoing nuclei remains intact. Jets are reconstructed down to $p_T = 15$ GeV using the anti-k_T algorithm with radius parameter, $R = 0.4$. Triple-differential cross sections, unfolded for detector response, are measured and presented using two sets of kinematic variables. The first set consists of the total transverse momentum (H_T), rapidity, and mass of the jet system. The second set uses H_T and particle-level nuclear and photon parton momentum fractions, x_A and z_γ, respectively. Results are compared with leading-order (LO) perturbative QCD calculations of photonuclear jet production cross sections, where all LO predictions using existing fits fall below the data in the shadowing region. Figure 5 shows the ratio between measured cross sections and predictions using PYTHIA 8 LO calculations and a variety of leading global nPDF fits. These comparisons demonstrate
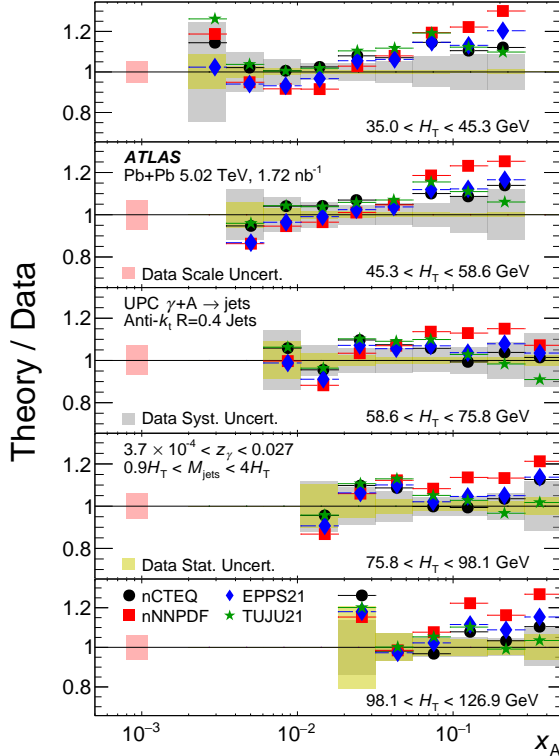

Fig. 5. Ratios of the triple-differential cross sections for photonuclear multi-jet production to theoretical predictions using several nPDF models as a function of x_A for different bins of H_T for events with struck parton energies in the kinematic range $3.7 \times 10^{-4} < z_\gamma < 0.027$ [14].

that no single fit describes the data in all kinematic regions. More detailed theoretical comparisons will allow these results to strongly constrain nPDF, and this data provides results from the LHC directly comparable to early physics results at the planned Electron–Ion Collider [15].

4.2. Search for magnetic monopoles

ATLAS conducted a search for highly ionizing magnetic monopoles in $262~\mu b^{-1}$ of UPC Pb+Pb data at $\sqrt{s_{NN}} = 5.36$ TeV collected in 2023 [16]. A new methodology that exploits the properties of clusters of hits reconstructed in the innermost silicon detector layers is introduced to study highly ionizing particles to separate monopole signal from beam-induced backgrounds. Also a new triggering concept is developed for efficient data recording for monopole searches. No significant excess above the background-only hypothesis, which is estimated using a data-driven technique, is observed. This is shown in Fig. 6. The gray solid line (black dashed line) represents observed (expected) limits, whereas the darker and lighter shaded bands around the expected limits represent the $\pm1\sigma$ and $\pm2\sigma$ intervals, respectively. Using a nonperturbative semiclassical model, upper limits at the 95%
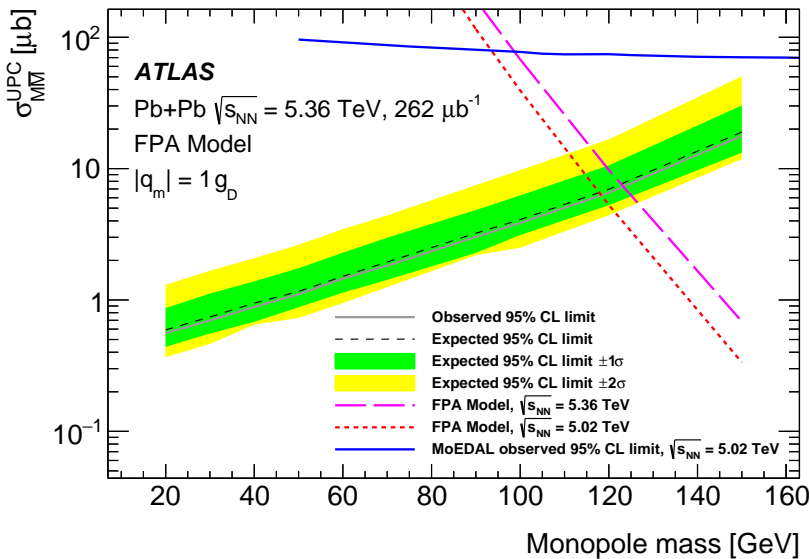

Fig. 6. Expected and observed upper limits on the monopole pair-production cross section in Pb+Pb UPC at $\sqrt{s_{NN}} = 5.36$ TeV for a single Dirac magnetic charge ($|q_m| = 1g_D$) and assuming the FPA model. The limits are compared with FPA model predictions (dashed lines) and the observed limits by MoEDAL for $|q_m| = 1g_D$ at $\sqrt{s_{NN}} = 5.02$ TeV (blue line) [16].

confidence level are set on the cross section for pair production of monopoles with a single Dirac magnetic charge ($|q_m| = 1g_{\mathrm{D}}$) in the mass range of 20–150 GeV. The search significantly improves on the previous cross-section limits from the MoEDAL experiment [17] for production of low-mass monopoles in Pb+Pb UPC.

5. Conclusions and outlook

The ATLAS experiment continues to deliver high-quality heavy-ion data. The reported precision results shed more light on properties of the QGP. With the first observation of top-quark production in Pb+Pb collisions at the LHC, ATLAS also provides unique hard probes of the medium, establishing the start of the heavy-ion programme with the heaviest quarks at the LHC. Ultra-peripheral collision data demonstrate the power to search for magnetic monopoles. With higher integrated luminosities of Run 3 Pb+Pb and reference *pp* collisions collected in 2023 and 2024, a wealth of new results is expected soon.

REFERENCES

[1] ATLAS Collaboration (G. Aad *et al.*), *J. Instrum.* **3**, S08003 (2008).

[2] ATLAS Collaboration (G. Aad *et al.*), *Phys. Rev. Lett.* **105**, 252303 (2010).

[3] ATLAS Collaboration, `arXiv:2412.15658 [nucl-ex]`.

[4] ATLAS Collaboration (G. Aad *et al.*), *Phys. Rev. Lett.* **133**, 252301 (2024).

[5] M. Gyulassy, X.-N. Wang, *Comput. Phys. Commun.* **83**, 307 (1994).

[6] B. Schenke, S. Jeon, C. Gale, *Phys. Rev. C* **82**, 014903 (2010).

[7] ATLAS Collaboration (G. Aad *et al.*), *Phys. Rev. C* **110**, 054912 (2024).

[8] ATLAS Collaboration (G. Aad *et al.*), *Phys. Rev. C* **111**, 044909 (2025).

[9] S. Cao, X.-N. Wang, *Rep. Prog. Phys.* **84**, 024301 (2021).

[10] ATLAS Collaboration (G. Aad *et al.*), *J. High Energy Phys.* **2024**, 101 (2024).

[11] ATLAS Collaboration, *Phys. Rev. Lett.* **134**, 142301 (2025).

[12] ATLAS Collaboration (M. Aaboud *et al.*), *Nature Phys.* **13**, 852 (2017).

[13] ATLAS Collaboration (G. Aad *et al.*), *Phys. Rev. Lett.* **123**, 052001 (2019).

[14] ATLAS Collaboration (G. Aad *et al.*), *Phys. Rev. D* **111**, 052006 (2025).

[15] A. Accardi *et al.*, *Eur. Phys. J. A* **52**, 268 (2016).

[16] ATLAS Collaboration (G. Aad *et al.*), *Phys. Rev. Lett.* **134**, 061803 (2025).

[17] MoEDAL Collaboration (B. Acharya *et al.*), *Nature* **602**, 63 (2022).